Physica 4D (1982) 366–393
North-Holland Publishing Company

CHAOTIC ATTRACTORS OF AN INFINITE-DIMENSIONAL DYNAMICAL SYSTEM

J. Doyne FARMER*
Dynamical Systems Group, Physics Dept., U.C. Santa Cruz, Santa Cruz, Ca. 95064, USA

Received 29 December 1980
Revised: 23 July 1981

We study the chaotic attractors of a delay differential equation. The dimension of several attractors computed directly from the definition agrees to experimental resolution with the dimension computed from the spectrum of Lyapunov exponents according to a conjecture of Kaplan and Yorke. Assuming this conjecture to be valid, as the delay parameter is varied, from computations of the spectrum of Lyapunov exponents, we observe a roughly linear increase from two to twenty in the dimension, while the metric entropy remains roughly constant. These results are compared to a linear analysis, and the asymptotic behavior of the Lyapunov exponents is derived.

Contents

1. Introduction

In 1963, Edward Lorenz observed aperiodic behavior in a three-dimensional dynamical system [1]. Lorenz's equations are such a severe truncation of the infinite-dimensional Navier–Stokes equations that their principal significance for fluid flow is metaphorical rather than predictive. Lorenz's observations do, however, present the possibility that the chaotic behavior observed in such an infinite-dimensional system might be caused by a finite-dimensional attractor. Numerical studies of the Lorenz equations and other low dimensional systems have provided considerable insight into the nature of deterministic yet random behavior observed in strange (chaotic) attractors, but the relationship between the chaotic attractors of these low dimensional systems and those of infinite dimensional systems has not yet been established. Although we cannot simulate the

*Present address: Center for Nonlinear Studies, MS 258, Los Alamos Scientific Laboratories, Los Alamos, New Mexico 87545, USA.

0167-2789/82/0000–0000/$02.75

Navier–Stokes equations properly, there are other infinite dimensional systems that can be simulated relatively simply.

In 1971, Ruelle and Takens [2] conjectured that the bifurcation sequence leading to turbulence should generically consist of fixed points, limit cycles, two-dimensional tori, and strange attractors, rather than the succession of quasiperiodic attractors of increasingly higher dimension suggested by Landau [3]. Experiments indicate that a temporal power spectrum of a fluid flow never contains more than a few irrationally related discrete frequency components. This supports the Ruelle–Takens theory, but the nature of the chaotic attractors in turbulent flows remains a mystery.

There are several rigorous results indicating that the attractors of many infinite-dimensional dynamical systems are of finite dimension and have a discrete spectrum of Lyapunov exponents. These results, including the work of Foias, Prodi, Teman [5, 6], Ladyzenskaya [7, 8], Mallet-Paret [9], and Ruelle [10] are briefly reviewed in section 6. Despite these results, very little is known about the structure of the chaotic attractors of infinite-dimensional systems and their behavior as parameters are changed. Many questions about bifurcation sequences to "fully developed" chaotic behavior remain to be answered, among them: How quickly does the dimension of chaotic attractors change as a control parameter (such as the Reynolds number in fluid flow) is varied? How steady is this change? Do the dynamics necessarily become more chaotic as the dimension of the attractor increases? (I.e., does the metric entropy increase?) Are the attractors of infinite-dimensional systems qualitatively similar to those of low-dimensional systems?

The answer to these and other questions requires a detailed characterization of the geometrical and statistical properties of an attractor. One of the main tools useful for this is the spectrum of Lyapunov characteristic exponents [11, 12, 13, 14]. Roughly speaking, the positive exponents measure the average rate of exponential spreading of nearby trajectories within the attractor, and the negative exponents measure the average rate of exponential convergence onto the attractor. One of our primary purposes here is to demonstrate how these exponents may be computed for infinite dimensional systems.

The dimension of an attractor is believed to be related to the spectrum of Lyapunov characteristic exponents, but this relationship is not yet certain. Two conjectures have recently been made, one by Kaplan and Yorke [15], and another by Mori [16]. The Kaplan–Yorke conjecture and the Mori conjecture give identical results for attractors of low-dimensional systems, and in this case, for many examples their predictions have been numerically demonstrated to be correct [17]. For higher-dimensional systems, however, their predictions may be drastically different. We use an infinite dimensional system to perform this test, and find that our results agree with the conjecture of Kaplan and Yorke.

This paper begins with a brief introduction to the characterization of chaotic dynamical systems in terms of dimension, metric entropy, and Lyapunov characteristic exponents, followed by a discussion on the extension of these concepts to infinite-dimensional systems, and a review of some pertinent rigorous results. We then compute these quantities for an infinite-dimensional differential delay equation originally studied by Mackey and Glass [18]. Our primary motivation for choosing this example is ease of simulation.

PART I: REVIEW OF GENERAL THEORY

2. Dimension

There are several different dimensions that can be used to describe dynamical systems and their attractors. In this section we present brief discussions of the phase space dimension, topological dimension, fractal dimension, in-

formation dimension, and embedding dimension.

The *phase space dimension* N is the number of independent real numbers that are needed to specify an arbitrary initial condition. The phase space dimension is a property of a dynamical system. The other dimensions we will discuss are generally properties of sets, but we will consider them in the context where they are properties of attractors.

Loosely speaking, an attractor is a subset of the phase space of a dissipative dynamical system, that "attracts" phase points from other regions of the phase space in the basin of the attractor. Once a phase point enters an attractor, it does not leave it. One convenient property observed in many numerical experiments is that almost every initial condition in a given basin yields the same time averages, and hence the same asymptotic probability measure [19]. Ruelle and Bowen [20] have proved that the Lebesgue measure of an attractor of a smooth flow is zero. This result suggests that perhaps the (suitably defined) dimension of an attractor is generally less than that of the phase space containing it. For trajectories on the attractor, this reduction of dimension brings about an accompanying reduction in the information needed to specify an initial condition. For the most general case, the number of phase variables needed to describe a trajectory is N, but for trajectories on an attractor this number may be less than N. The various dimensions defined below seek to make the concepts of "information required to specify an initial condition" and "degrees of freedom on the attractor" more precise.

One of the oldest notions of dimension is that of *topological dimension*, developed by Poincaré, Brouwer, Menger, Urhsohn, and others [21]. The topological dimension is an integer that makes rigorous the notion of the number of "locally distinct directions" in a set. Since we are not going to make very much use of this concept, and since the definition is somewhat involved, we refer the reader to Hurewicz and Wallman [21].

For a dynamical system with an N-dimensional phase space, let $n(\epsilon)$ be the number of N-dimensional balls of radius ϵ required to cover an attractor. The capacity, or *fractal dimension* [22] is

$$D_F = \lim_{\epsilon \to 0} \frac{\log n(\epsilon)}{|\log \epsilon|}. \tag{1}$$

When a set is "simple", for example, a limit cycle or a torus, the fractal dimension is an integer equal to the topological dimension. The classical example of a set with a noninteger fractal dimension is Cantor's set. (Sets whose fractal dimension exceeds their topological dimension are called "fractals" by Mandelbrot [22].) To construct Cantor's set, delete the middle third of a line segment, then delete the middle third of each remaining piece, and so on. The fractal dimension is log 2/log 3. Smale's horseshoe [23], and many other constructions of chaotic mappings have an analogous structure; numerical simulations of dynamical systems with chaotic attractors, such as the example studied by Henon [24], indicate that such structure occurs for chaotic attractors.

To understand the physical meaning of the fractal dimension, suppose that the N coordinates of a dynamical system are measured by an instrument incapable of resolving values separated from each other by less than an amount ϵ. For convenience, assume that all the coordinates are measured with equal precision. The instrument thus induces a partition that divides the phase space into elements of equal volume. To an observer whose only a priori knowledge is a list of the $n(\epsilon)$ partition elements that cover the attractor, the amount of new information gained upon learning that the phase point describing the state of the system is in a given partition element is $\log n(\epsilon)$. If the resolution of the measuring instrument is in-

creased, the number of partition elements needed to cover the attractor goes up roughly as ϵ^{-D_F}. Thus, assuming that all partition elements are equally likely, for small ϵ, the amount of new information obtained in a measurement is roughly

$$I = \log n(\epsilon) \approx D_F |\log \epsilon|. \tag{2}$$

For most chaotic attractors, however, the elements of a partition do not have equal probability. Assume that each element of a partition has probability P_i. On the average, the amount of information gained in a measurement by an observer whose only a priori knowledge is the distribution of probabilities $\{P_i\}$ is

$$I(\epsilon) = -\sum_{i=1}^{n(\epsilon)} P_i \log P_i. \tag{3}$$

This leads to a generalization of the fractal dimension:

$$D_I = \lim_{\epsilon \to 0} \frac{I(\epsilon)}{|\log \epsilon|}. \tag{4}$$

This dimension was originally defined by Balatoni and Renyi [25] in 1956. They refer to it simply as the "dimension of a probability distribution". In order to avoid confusion with other dimensions, however, we will refer to this as the *information dimension*. Since $\log n(\epsilon) \geq I(\epsilon)$, the fractal dimension D_F is an upper bound for the information dimension D_I. We will refer to sets whose fractal dimensions exceed their information dimension as "probabilistic fractals". To construct an example, begin with a uniform probability distribution on the interval, and rather than deleting the middle third, make it less probable than the outer thirds, Then repeat this process for each third, and so on. The limiting set has a fractal dimension of one, but an information dimension less than one. (See ref. 26.)

For an attractor of information dimension D_I, the amount of information gained in a measurement made using instruments of resolution ϵ is

$$I(\epsilon) \approx D_I |\log \epsilon|. \tag{5}$$

For a more complete discussion of the information dimension in the context of dynamical systems, see ref. 26. Work on this topic has also been done recently by Yorke [27].

Thus, the notion of "information required to specify an initial condition" can be described in terms of the information dimension. The notion of "degrees of freedom", however, is perhaps most appropriately described by another dimension, which we will refer to as the *embedding dimension*. An *embedding* is a smooth map $f: X \to Y$ that is a diffeomorphism from a smooth manifold X to a smooth submanifold Y. Define the embedding dimension M of an attractor as the minimum dimension of a subset of Euclidean space into which a smooth manifold containing the attractor can be embedded. M variables are sufficient to conveniently and uniquely specify a point on an attractor, and it is in this sense that the embedding dimension is the number of degrees of freedom.

If there is a smooth manifold containing the attractor of dimension m, then the Whitney embedding theorem guarantees that its embedding dimension will be $M \leq 2m + 1$. Unfortunately, chaotic attractors are not in general smooth manifolds, and a relationship between the embedding dimension and other dimensions (e.g. fractal) of attractors has not yet been proven.

Note that the fractal dimension, information dimension, and embedding dimension all require a metric on the phase space. The information dimension, in addition, requires a probability measure.

3. Metric entropy

One of the essential differences between chaotic and predictable behavior is that chaotic trajectories continually generate new information, whereas predictable trajectories do not. The metric entropy makes this notion precise. In addition to providing a good definition of "chaos", the metric entropy provides a quantitative way to describe "how chaotic" a dynamical system is.

Suppose a phase space is partitioned into n elements, each of which is assigned a symbol s_i. Consider a sequence $S_j(m)$ of m successive measurements made at a time interval Δt, $S_j(m) = s_{i_1}, s_{i_2}, \ldots, s_{i_m}$. Let $P(S_j(m))$ be the probability of the sequence $S_j(m)$, normalized so that $\Sigma_j P(S_j(m)) = 1$. The amount of information contained in sequences of length m is

$$I_m = -\sum_j P(S_j(m)) \log P(S_j(m)). \tag{6}$$

Taking the maximum value over all possible partitions β finite, the metric entropy is the information per unit time in a sequence of measurements,

$$h_\mu = \sup_\beta \frac{I_m}{m\Delta t}. \tag{7}$$

For predictable dynamical systems, eventually new measurements provide no further new information, and the metric entropy is zero. For chaotic dynamical systems new measurements continue to provide new information, and the metric entropy is positive.

As defined here, the metric entropy depends on the set of probabilities $P(S_j(m))$. This in turn may depend on the choice of initial condition. (An initial point on an unstable limit cycle, for example, may give a qualitatively different sequence of measurements than a point not on a limit cycle.) Nevertheless, we will assume that almost every point within the basin of an attractor yields the same limiting value for h (almost every in the sense of Lebesgue measure). With this assumption the metric entropy can be considered to be a property of an attractor.

More complete discussions of the metric entropy can be found in refs. 20, 26, and 28 to 33.

4. Lyapunov exponents and their relation to entropy and dimension

The spectrum of Lyapunov characteristic exponents provides a summary of the local stability properties of an attractor. In addition, there is good evidence that the metric entropy and information dimension of an attractor can be expressed in terms of the spectrum of Lyapunov exponents. The spectrum of Lyapunov exponents will be our primary tool for studying attractors. In this chapter we define the Lyapunov exponents, and review the conjectures and theorems relating the spectrum of Lyapunov exponents to dimension and entropy.

The stability properties of a system are determined by behavior under small perturbations. A system can be stable to perturbations in certain directions, yet be unstable to perturbations in others. All possible perturbations can be examined simultaneously by following the evolution of an ensemble of points that is initially contained in a small N-dimensional ball, where N is the phase space dimension. This should motivate the following definition of the spectrum of Lyapunov exponents:

Consider a dynamical system of dimension N. Imagine an infinitesimal ball that has radius $\epsilon(0)$ at time $t = 0$. As this ball evolves under the action of a nonuniform flow it will distort. Since the ball is infinitesimal, however, this change in shape is determined only by the linear part of the flow, and it remains an ellipsoid as it evolves. Call the principal axes of this ellipsoid at time t $\epsilon_i(t)$. The spectrum of Lyapunov exponents λ_i for a given starting position is

$$\lambda_i = \lim_{t\to\infty} \lim_{\epsilon(0)\to 0} \frac{1}{t} \log \frac{\epsilon_i(t)}{\epsilon(0)}. \tag{8}$$

There are N Lyapunov exponents in the spectrum of an attractor of an N-dimensional dynamical system. Positive Lyapunov exponents measure average exponential spreading of nearby trajectories, and negative exponents measure exponential convergence of trajectories onto the attractor. Note that the sum of the Lyapunov exponents is the average divergence, which for a dissipative system, must always be negative.

For sufficiently dissipative systems, there are many examples where numerical evidence indicates that the values of the Lyapunov exponents are the same for almost every point in the basin of an attractor. In these cases, the spectrum of exponents may be taken to be a property of an attractor, independent of initial condition. Since this assumption seems to be justified for our example, we will assume throughout that this is the case.

We will always assume that the Lyapunov exponents are arranged in decreasing order. The qualitative stability properties of an attractor can then be conveniently summarized by indicating +, 0, or −, according to the sign of each exponent. Thus [+, 0, −], for example, might indicate a chaotic attractor in a three-dimensional phase space, with (on the average) exponential expansion on the attractor, neutral stability along the flow, and exponential contraction of trajectories onto the attractor. Note that for continuous flows, attractors that are not fixed points always have at least one exponent equal to zero, since on the average points along a trajectory confined to a compact set can neither separate nor merge.

4.1. Relation to dimension

To gain an intuitive understanding of the relation between dimension and the spectrum of Lyapunov exponents, it is easiest to begin with simple attractors. If an attractor has a spectrum [−, −, −, . . .], since the flow is contracting in every direction, the attractor is a fixed point, and has dimension zero. A spectrum [0, −, . . .] indicates that the attractor is a limit cycle, of dimension one. Similarly, a spectrum [0, 0, −, . . .] indicates that the attractor is a two-torus.

For simple attractors such as those above, the notion of dimension is unambiguous, and the relationship to the spectrum of Lyapunov exponents is clear. Chaotic attractors, in contrast, can be fractals [22], or probabilistic fractals [26]; this complicates the relationship between the dimension and the spectrum of exponents. As discussed in section 2, at least four distinct dimensions can be assigned to a chaotic attractor. It is a nontrivial problem even to determine which of these dimensions should be related to the spectrum of Lyapunov exponents.

Two conjectures have recently been put forth to relate the dimension to the spectrum of Lyapunov exponents. Kaplan and Yorke [15] define a quantity they call the Lyapunov dimension

$$D_L = j + \frac{\sum_{i=1}^{j} \lambda_i}{|\lambda_{j+1}|}, \tag{9}$$

where j is the largest integer for which $\lambda_1 + \cdots + \lambda_j \geq 0$. Kaplan and Yorke conjecture that the Lyapunov dimension is equal to the information dimension [27]. Mori [16], in contrast, has conjectured that the fractal dimension D_F of an attractor is

$$D_F = d + \frac{\sum_{i=1}^{k} \lambda_i^+}{\sum_{i=1}^{l} |\lambda_i^-|}, \tag{10}$$

where d is the number of non-negative exponents, k is the number of positive exponents λ_i^+, and l is the number of negative exponents λ_i^-. For continuous systems of phase space dimension three or less, or discrete sys-

tems of dimension two or less, these two formulas give the same result. For larger dimensional systems, their predictions may differ. This is especially apparent in infinite dimensions. In this case the number of exponents is infinite, and their values decrease monotonically, so the denominator in eq. (10) is infinite. Therefore, Mori's formula predicts that the fractal dimension D_F of an infinite dimensional dynamical system is always an integer, i.e. $D_F = d$. In contrast, Kaplan and Yorke's formula depends only on the largest $j+1$ exponents, rather than the entire spectrum, so that their formula does not necessarily distinguish infinite- from finite-dimensional systems.

Frederickson, Kaplan, and Yorke [34] have simulated several discrete mappings, and computed their Lyapunov dimension. They do not compute the information dimension, but they show that it agrees qualitatively with the Lyapunov dimension. Russel et al. [17] have calculated the fractal dimension directly from the definition for a few examples, and compared it to that predicted from the exponents. They find good agreement, but unfortunately none of the cases they studied are of sufficiently large dimension to distinguish between Mori's conjecture and the Kaplan–Yorke conjecture. Our example does distinguish between these two conjectures: We find non-integer dimensions according to the Kaplan–Yorke conjecture. (See section 8.)

4.2. *Relation to metric entropy*

We defined the spectrum of Lyapunov exponents in terms of the evolution of a small ball. This ball can also be considered to represent an ensemble of points, modeling the uncertainty in an initial measurement. The discussion about stability can then be rephrased in the language of information theory. The average initial rate at which the information contained in a measurement corresponding to a small ball decays corresponds, at least for smooth measures, to the metric entropy [35]. If a fine, uniform partition is made of the phase space, the initial exponential rate at which new partition elements are filled by the evolving ensemble of points is determined by the positive Lyapunov exponents. The preceding discussion is intended to motivate the following relationship:

$$h_\mu = \sum_{i=1}^{k} \lambda_i^+. \tag{11}$$

h_μ is the metric entropy, and λ_i^+ are the positive Lyapunov exponents. Pesin [36] originally proved this for flows with an absolutely continuous invariant measure, and it was also proved by Ruelle and Bowen [20] for Axiom-A flows. This relationship is also supported by numerical computations on one-dimensional mappings [37]. For the calculations performed here, we will assume that the metric entropy can be computed using eq. (11). We previously defined a chaotic attractor as any attractor with positive metric entropy; according to this relationship, a chaotic attractor is also any attractor with a positive Lyapunov exponent.

5. Simulating infinite-dimensional dynamical systems

A dynamical system is infinite dimensional if an infinite set of independent numbers are required to specify an initial condition. For example, to describe the state of a classical fluid at any given time the velocity and possibly other functions must be specified at an infinite number of spatial points. The example we will study in this paper is a delay differential equation of the form

$$\dot{x}(t) = F(x(t), x(t-\tau)), \tag{12}$$

where τ is a delay time. To calculate $x(t)$ for times greater than t, a function $x(t)$ over the interval $(t, t-\tau)$ must be given. Thus, equations of this type are infinite dimensional.

To simulate the behavior of infinite-dimensional systems on a computer it is necessary to approximate the continuous evolution of an infinite-dimensional system by a finite number of elements whose values change at discrete time steps. In this manner a continuous infinite-dimensional dynamical system is replaced by a finite-dimensional iterated mapping. There is no unique method for doing this. The simulation of partial differential equations, for example, may be accomplished by conversion to a set of ordinary differential equations for the Fourier modes, or by various methods that use the values of the spatial functions at a finite number of lattice points. With either type of method, a variety of different integration schemes are possible, each corresponding to a different iterated mapping.

Note: To simulate on a digital computer, in addition to the finite dimension approximation, the continuous variable must be approximated by a finite number of states. We will not deal with the ramifications of this latter assumption here. (See ref. 37.)

For nonlinear equations that cannot be solved analytically, there is no rigorous method to make certain that a simulation is faithful to the equations. There are, however, certain indicators: The behavior of the simulated system must agree for any cases where analytic solutions are known; the behavior of the simulation should converge as the resolution of the simulation increases; and, simulations by several different "proper" methods should all give similar results. We will refer to any simulation scheme that satisfies the above criteria as a *proper simulation*. It is common practice to assume that proper simulations accurately represent the equations being simulated; this assumption will be made here.

The existence, uniqueness, and general properties of the spectrum of Lyapunov exponents in infinite dimensions are not trivial problems. Some aspects of these questions are reviewed in section 6. Simulations, however, are *necessarily* finite dimensional, so that the theory of finite dimensional dynamical systems can be applied [38]. In this paper, we apply the criteria given above, hope that our simulation is therefore representing properties of the continuous equation, and compute the spectrum of Lyapunov exponents of the simulation. When the resolution of our simulation is refined so that the dimension of the simulation goes from N to $2N$, for N sufficiently large, we find that the first N exponents of the refined system are approximately the same as those of the original N-dimensional system. (Recall that an N-dimensional dynamical system has exactly N exponents.) The fact that this procedure converges for a few test cases at very high resolution provides the justification for our assumption that the spectrum of exponents we compute is approximately that of the infinite dimensional equations.

As will be more apparent from the discussion in section 9, a computation of the largest m exponents of an N-dimensional proper simulation is equivalent in computational difficulty to the iteration of an mN-dimensional mapping. Fortunately, the largest m exponents may be computed without computing the $N-m$ smaller exponents.

In general, to gain a geometric picture of an N-dimensional dynamical system, all N coordinates of the system must be taken into account. However, if an attractor has an embedding dimension $M < N$, only M variables are needed to determine a trajectory on the attractor. For example, the existence of a stable fixed point may be seen with only one coordinate; a picture of a limit cycle can be drawn with only two, and so on. Any dynamical visualization entails this sort of projection of the infinite (or large N)-dimensional dynamics onto some lower dimensional space. In this paper we will

make use of projections to study the geometry of the attractors we are interested in. Just as there is some arbitrariness in the integration scheme used to simulate a dynamical system, so the projections used to study a system are also somewhat arbitrary. After testing several possibilities in each case (and getting equivalent results) we will assume that the properties we see are independent of the projection we use.

6. Review of rigorous results for infinite-dimensional systems

There are several theoretical questions that have simple answers for finite-dimensional dynamical systems, but become more delicate in the context of infinite-dimensional systems. For example: Are the attractors of infinite-dimensional systems generally of finite dimension? Does the spectrum of Lyapunov exponents exist, and if so, is it discrete? Rigorous results that address these questions will be reviewed in this section.

The qualitative theory of dynamical systems used by Ruelle and Takens for their picture of turbulence applies only to finite-dimensional systems, but they argued that their finite dimensional results would hold for many infinite-dimensional dynamical systems by virtue of the *Center Manifold Theorem*. This theorem states that when a stable fixed point of an infinite dimensional dynamical system turns unstable with a pair of eigenvalues acquiring positive real part as a parameter is varied, there exists a finite dimensional invariant attracting center manifold [38].

There are other mathematical results that give credence to the idea that chaotic behavior in infinite dimensional dynamical systems might be explained by finite-dimensional chaotic attractors. Ladyzhenskaya [7, 8] has generalized results of Foias, Prodi, and Temam [5, 6] to show that time-dependent solutions of the Navier–Stokes equations are homeomorphic to a compact subset of $\mathbf{R}^m$ for m sufficiently large. Using slightly different techniques, Mallet-Paret [9] has proven the following theorem:

Theorem (Mallet-Paret [9]). Let H be a separable Hilbert space, and suppose

$$A \subset U \subset H,$$

where A is compact and U is open. Let

$$T : U \to H$$

be C^1 (have a continuous Frechet derivative) and be "negatively invariant," that is $T(A) \supseteq A$. Suppose further there is a linear subspace $C \subset H$ with

$$|DT(x)|_C| < 1, \quad \text{for all } x \in A \text{ and codim } C < \infty.$$

Then the topological dimension of A is finite.

Mallet-Paret uses this theorem to prove that the attractors of delay equations such as the example we study here are finite dimensional. Unfortunately, neither this theorem nor the results of Foias, Prodi, Temam, and Ladyzhenskaya set any bounds on the dimension of the attractor.

The existence of Lyapunov exponents in finite-dimensional dynamical systems has been known since Oseledec [11]. Under certain assumptions, Ruelle [10] has recently proved the existence of Lyapunov exponents for infinite-dimensional dynamical systems. For the cases he considers, Ruelle's theorems assure us of a discrete spectrum of Lyapunov exponents, and moreover of a finite number of positive Lyapunov exponents.

PART II: CASE STUDY

7. Phenomenology of an infinite-dimensional example

The equation we will study here is a delay differential equation of the form

$$\frac{dx(t)}{dt} = F(x(t), x(t-\tau)). \tag{13}$$

In order to be well posed, a problem in this form needs as initial data the value of the function $x(t)$ over an interval of length τ. Delay equations such as eq. (13) describe systems in which a stimulus has a delayed response. There are many practical examples from control theory, economics, population biology, and other fields.

The example used for this investigation is a model of blood production due to Mackey and Glass [18]:

$$\dot{x} = \frac{ax_\tau}{1+x_\tau^c} - bx. \tag{14}$$

x_τ is the variable at a delayed time, i.e. $x_\tau = x(t-\tau)$. In this study we keep the parameters a, b, and c fixed at $a = 0.2$, $b = 0.1$, and $c = 10$, and vary the delay time τ. $x(t)$ represents the concentration of blood at time t, when it is produced, and $x(t-\tau)$ is the concentration when the "request" for more blood is made. In patients with leukemia, the time τ may become excessively large, and the concentration of blood will oscillate, or if τ is even larger, the concentration can vary chaotically, as demonstrated by Mackey and Glass. The qualitative behavior of this equation is quite similar to a model for the population of whales studied by May [40]. See also the two variable discrete delay equation studied by Shibata and Saito [41].

We will now describe some of the changes that occur in the qualitative nature of the attractors as the parameter τ is varied. A linear stability analysis shows that, with a, b, and c as given above, there is a stable fixed point attractor for $\tau < \tan^{-1}(-4)/0.4 = 4.53$. For $4.53 < \tau < 13.3$, numerical simulations show that there is a stable limit cycle attractor. At $\tau = 13.3$, the period of this limit cycle doubles, initiating a period doubling bifurcation sequence [42] that reaches its accumulation parameter at $\tau = 16.8$. For $\tau > 16.8$ numerical simulations show chaotic attractors at most parameter values, with some limit cycles interspersed in between.

To study the qualitative nature of the attractors of this dynamical system, we will employ a variety of methods. We begin using two of the more common methods, namely to display a representative portion of a time series, fig. 1, and the power spectrum, shown in fig. 3. In addition, we show a few phase plots in fig. 2,

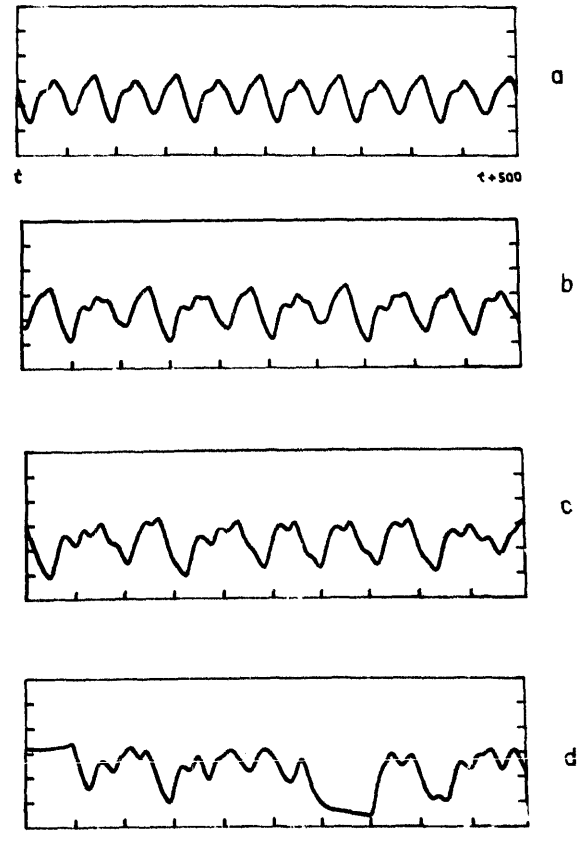

Fig. 1. Representative samples of time series generated using eq. (14), with $a = 0.2$, $b = 0.1$, $c = 10$. (a) $\tau = 14$. (b) $\tau = 17$. (c) $\tau = 23$. (d) $\tau = 300$, where τ is the delay parameter. A constant function was used as an initial condition; before plotting, the equation was iterated long enough to let transients die out. The total time span shown in each frame is 500 time units.

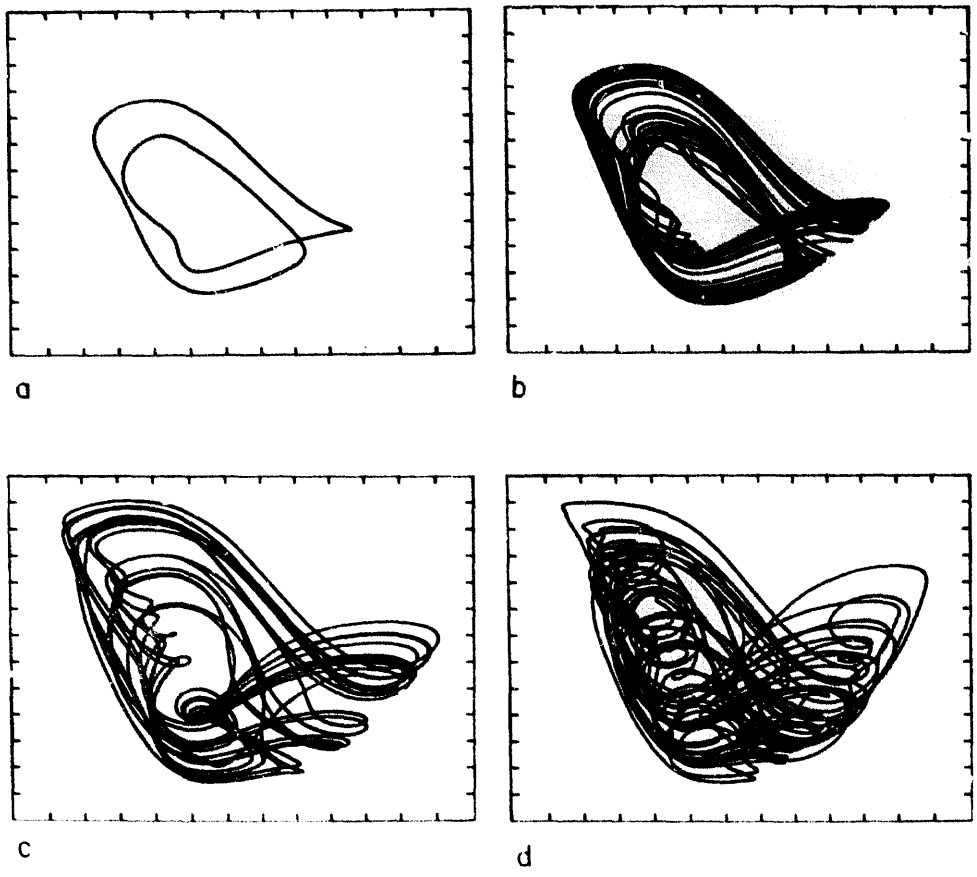

Fig. 2. Phase plots obtained by plotting $x(t)$ vs. $x(t-\tau)$, after letting transients relax. The parameter values are the same as those of (a), (b), (c) and (d) of fig. 1.

made by plotting $x(t)$ against $x(t-\tau)$. (Note that the choice of $x(t-\tau)$ as the other phase variable is arbitrary; $x(t-t')$ could equivalently be used, where t' is an arbitrary time delay.) As we shall see, these methods are adequate to distinguish periodic behavior from chaotic behavior, but are inadequate to make a sharp distinction between the properties of qualitatively different chaotic behavior; this distinction requires a computation of the spectrum of Lyapunov exponents.

Let us begin by comparing fig. 1a, a periodic time series, to fig. 1b, a chaotic series near the "onset". Although the chaotic series seen in fig. 1b is approximately periodic, a careful examination reveals that it is not. This is more apparent in the phase plots: The limit cycle forms a closed loop, but the orbit of the chaotic attractor appears to fill out a continuous band. Similarly, the power spectrum of the limit cycle, fig. 3a, is composed of delta functions (the small amount of broadening is due to the finite length of the time record). In contrast, although the power spectrum of the chaotic attractor, fig. 3b, contains fairly sharp peaks, it also has broadband components. Note: As we will see later (fig. 4a), this attractor is actually a two band, semiperiodic chaotic attractor [43, 44, 45] associated with the period doubling sequence. As shown in ref. 46, the power spectra of these attractors always contain sharp peaks, since they are approximately phase coherent [47].

An examination of the time series and power spectra shows that the chaotic attractors at larger values of τ contain motion on more different time scales than the "onset" chaos at $\tau = 17$. The phase plots at larger values of τ are con-

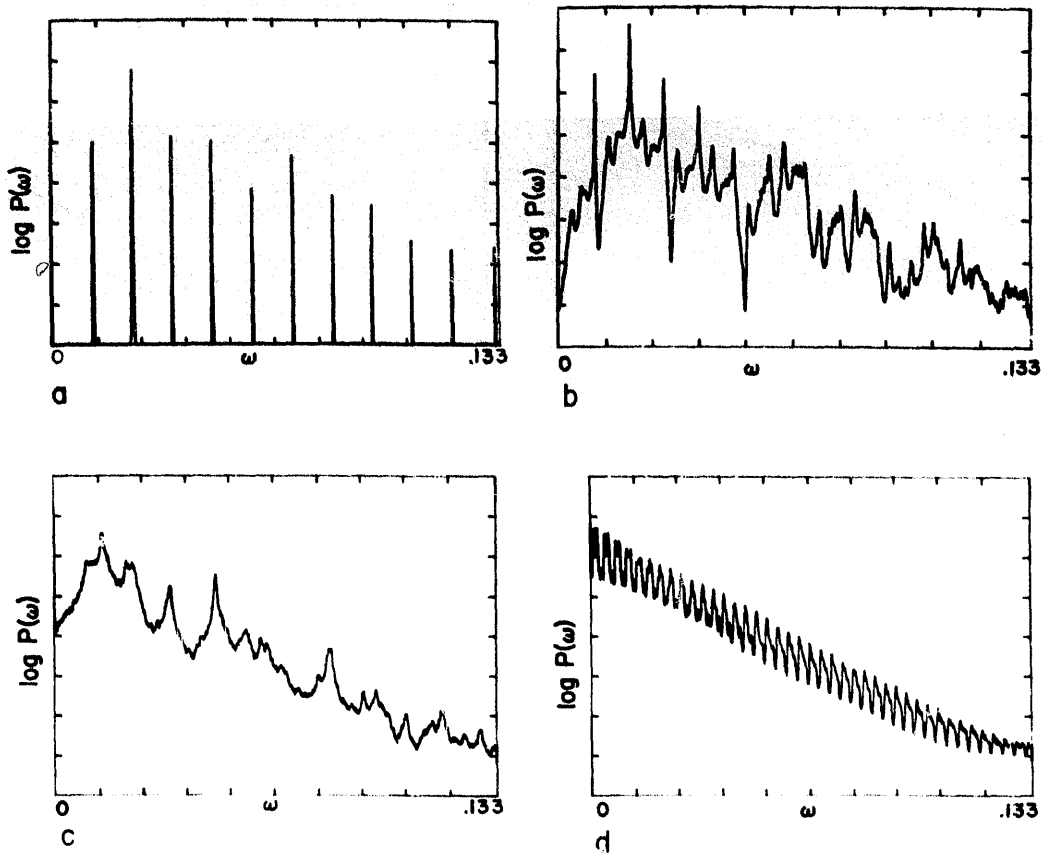

Fig. 3. Power spectra for the examples used in fig. 1 and fig. 2. Each spectrum is constructed with 100 averages, each of 4096 samples taken at intervals $\Delta t = 3.75$. These plots are on a semilog scale, and cover 8 orders of magnitude.

siderably more complicated, and the spectra contain less pronounced peaks. At $\tau = 300$, the motion is quite aperiodic, and the spectrum shows an exponentially decaying envelope, with a curious modulation superimposed on it. (We were unable to isolate any numerical artifacts that might cause this modulation; insofar as we were able to determine, it is a real effect.)

Several important questions about these attractors remain unanswered, for example: What is the dimension of these chaotic attractors? A more detailed understanding requires an examination of Poincaré sections, or, if this fails (as it will if the dimension of the attractor is greater than three), a computation of the spectrum of Lyapunov exponents. This is done in the following sections.

Note: The numerical methods used to obtain the results presented in this paper are discussed in the appendix.

8. Taking sections to visualize fractals in function space

In this section we demonstrate how phase variables may be arbitrarily chosen (within limits), and used to construct a cross section picture of an attractor. We use this method, together with computations of the fractal dimension and the spectrum of Lyapunov exponents (see section 9), to demonstrate that the Kaplan–Yorke conjecture (eq. (9)) gives a reasonable approximation to the dimension, whereas the Mori conjecture (eq. (10)) does not.

To see the geometrical structure of an attrac-

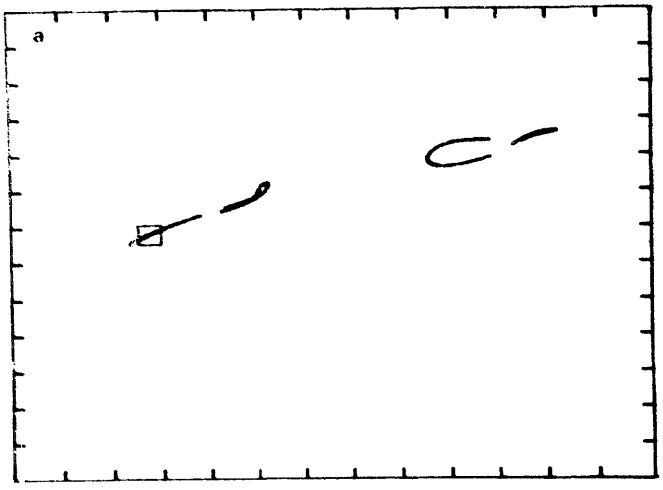

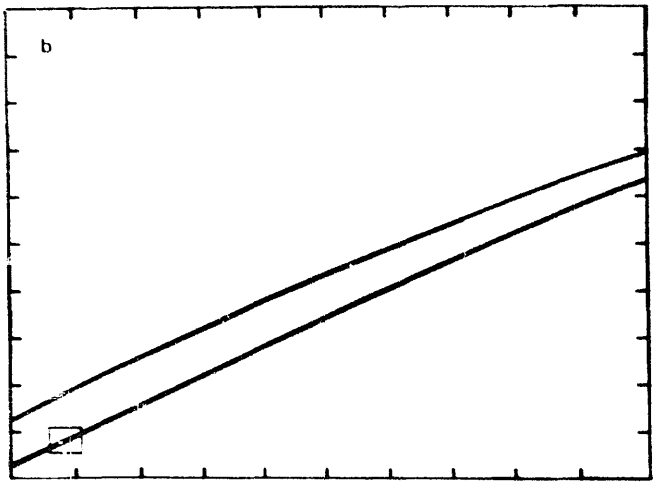

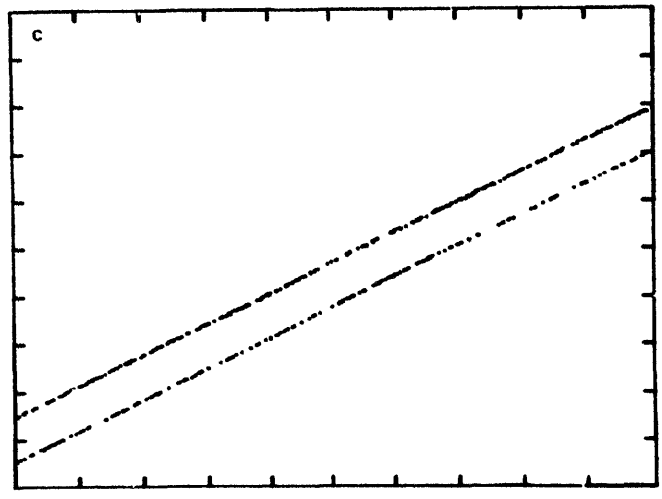

Fig. 4. A cross section of the chaotic attractor for $\tau = 17$. (See figs. 1a, 2a, and 3a.) These sections are constructed by plotting $x(t-\tau_1)$ vs. $x(t-\tau_2)$ whenever $x(t) = 0.85$, with $\tau_1 = 10$, and $\tau_2 = 20$. In this figure, as well as figs. 5–7, the blowups shown in (b) and (c) are constructed by plotting only those points that lie within the box indicated in figs. (a) and (b). The number of points indicated is the total number of points generated, rather than the number of points that actually appear in the figure. The dimension D_F listed in each case is the fractal dimension computed directly from the definition, as described in the text. This should be compared with the dimensions computed from the spectrum of Lyapunov exponents, shown in table I. Fig. 4a contains 1500 points, while (b) and (c) were constructed from 200,000 points. For this figure, $D_F = 1.13$.

tor, a picture can be made of the intersection of the attractor with a transverse surface. In order to do this, it is necessary to choose phase variables. For example, we chose $x_1 = x(t)$, $x_2 = x(t-\tau_1)$, $x_3 = x(t-\tau_2)$, with $\tau_1 = 10$, and $\tau_2 = 20$. Starting from an (arbitrarily chosen) constant initial function, after integrating long enough to insure that the trajectory was close to the attractor, we made a plot of x_2 vs. x_3 whenever $x_1 = 0.85$. For the limit cycle shown in fig. 2a, for example, the picture obtained consists of four dots, corresponding to the points where the curve cuts through the plane defined by $x_1 = 0.85$.

Fig. 4a shows a cross section constructed for $\tau = 17$, a parameter value close to the initial transition to chaos at $\tau = 16.8$. This attractor shows the characteristic band structure, or semiperiodicity [41, 43, 44], that occurs on the chaotic side of period doubling sequences. Four strips, two with trajectories coming out of the plane, and two with trajectories into the plane, can be seen in the figure. Figs. 4b and 4c are blowups of pieces of this cross section at successively greater resolution. This chaotic attractor has a simple, self similar microscopic structure, reminiscent of Henon's map [22], except that the structure is simpler. At each scale of resolution only two sheets are discernible to the eye. A careful perusal of fig. 4c suggests that the top sheet is slightly more probable than the bottom sheet. Assuming that this structure is also perpetuated on all scales, this indicates that this attractor is a probabilistic fractal. (See section 2 and ref. 26.) However, since the probabilities of the two sheets are not drastically different, the fractal and information dimension should be fairly close in value.

In order to test the Kaplan–Yorke and Mori conjectures, we ideally should compute both the fractal dimension and the information dimension directly from their definitions, and compare the values obtained to the values predicted from the spectrum of Lyapunov exponents using eqs. (9) and (10). We made direct computations only of the fractal dimension. The information dimension is a lower bound on the fractal dimension, so that the Kaplan–Yorke conjecture can be considered to give a lower bound on the fractal dimension. For the two cases where we made an accurate computation of the fractal dimension, the agreement we find between the fractal dimension and the computations of Kaplan and Yorke's Lyapunov dimension indicates that the information dimension and the fractal dimension are quite close, so that our failure to compute the information dimension is not a serious problem.

To directly compute fractal dimension, we divide the region of the cross section containing the attractor into a grid of resolution $1/\epsilon$ by $1/\epsilon$, where $1/\epsilon$ varies from 64 to 1024 in powers of two. We integrate the equation under study to accumulate at least 10^5 points on the cross section. At each level of resolution the number n of squares of the grid that are filled by points of the attractor is counted. The estimated dimension of the cross section is the slope of $\log n$ vs. $\log 1/\epsilon$.

Since the attractor is continuous along the flow, the fractal dimension of the attractor is the fractal dimension of the cross section plus one. For reasons of convenience, however, for this study we used a two dimensional projection of the (infinite dimensional) cross section, as shown in figs. 4–7. If the dimension of the attractor exceeds three, two dimensional squares will not form an adequate cover of the section, and the computed result is necessarily a lower bound.

We assume that fractal dimension measured in this way is independent of the choice of cross section. A few numerical experiments that we have performed support this, as does the agreement between predicted and measured values, but we do not know of any results that say that this will be true for the general case.

Table I contains estimates of the dimension made at four values of τ. In order to estimate the accuracy of these estimates, the dimension was computed twice, once with $n(1/1024)$, and again without it. The quoted error bars are the difference between these two estimates.

For $\tau = 23.8$ and $\tau = 30$, for small values of ϵ it was not feasible to generate enough data points to get n to converge. Since this problem becomes worse as ϵ decreases, this effect systematically lowers the estimate of the dimension. Thus, for these values of τ the results given in table I are merely lower bounds. Note that if the Kaplan–Yorke conjecture is correct, the dimension of the attractor exceeds three for these parameter values, and the computed result is a lower bound in any case.

For fig. 4a, we found the largest Lyapunov exponents in the spectrum of this attractor to be [0.007, 0, −0.071, −0.15, ...]. (See section 9 for the method of computation of the Lyapunov exponents.) A direct computation of the fractal dimension of the attractor gives $D_F = 2.13$. This agrees to experimental accuracy with the Lyapunov dimension computed from the Kaplan–Yorke conjecture (see table I). This does not agree with the integer value 2 predicted by Mori's conjecture.

A single cross section does not do justice to the complexity of the global structure of this attractor. By making many parallel cross sections covering the attractor, the entire attractor

TABLE I
A comparison of the fractal dimension computed directly from the definition, to the dimension calculated from the spectrum of Lyapunov exponents according to conjectures by Kaplan and Yorke and Mori.

Delay	Dimension from definition eq. (1)	Dimension from Kaplan–Yorke eq. (9)	Dimension from Mori eq. (10)
17	2.13 ± 0.03	2.10 ± 0.02	2
23	2.76 ± 0.06	2.82 ± 0.03	2
23.8	> 2.8	3.04 ± 0.03	2
30	> 2.94	3.58 ± 0.04	3

Fig. 5. See the caption to fig. 4, and table 1. The delay parameter $\tau = 23$, and $D_F = 1.76$. Fig. 5a contains 10,000 points; (b) and (c) were constructed from a total of 760,000 crossings of the section.

can be reconstructed. When this was done for $\tau = 17$, forty different cross sections were needed to make it possible to smoothly interpolate between the sections. The section shown in fig. 4 is one of the simpler cases. For many cross sections, the sheetlike structures overlap, indicating that this attractor cannot be embedded in three dimensions, at least with this choice of coordinates. Several different values of τ_1 and τ_2 were tried, but none of these proved adequate for a three dimensional embedding. One interpretation is that, although this attractor has a fractal dimension of approximately 2.13, the embedding dimension $M \geq 4$.

As the delay parameter is increased, for most parameter values the dimension increases, and the attractor generally becomes more complicated. A cross section of the attractor at $\tau = 23.0$, where the dimension is the order of 2.8, is shown in fig. 5. A glance suggests sheetlike structure, but a closer examination reveals stray points. This is particularly apparent in fig. 5c. We suggest the following interpretation: All these points lie on sheets, but some sheets are much more probable than others. This theory is borne out by making several plots of the same section, with differing numbers of points on them (not shown here). As the number of points is increased, points that do not appear to lie on sheets gain neighbors that suggest sheets. Nevertheless, new points appear elsewhere that do not appear to lie on sheets, indicating sheets that are even less probable. (As argued in ref. 26, this inequity of probability is to be expected for a chaotic attractor.) At the level of resolution obtainable for these numerical experiments, it is not possible to see self-similar scaling for this attractor; blow-ups of different pieces give pictures that are quite different in appearance.

When τ is raised to 23.8, the Lyapunov dimension (eq. (10)) of the attractor exceeds three, and a section of the attractor should fill in (fig. 6). There are indications that this will eventually happen as the number of points is increased, but because of the unequal distribution of probabilities the number of points required to see this take place at the resolution of the plotter is prohibitively large.

The attractor at $\tau = 23.8$ only has two nonnegative exponents, so there are only two directions in which the phase space is not contracting. However, according to the Kaplan and Yorke conjecture, its dimension exceeds three.

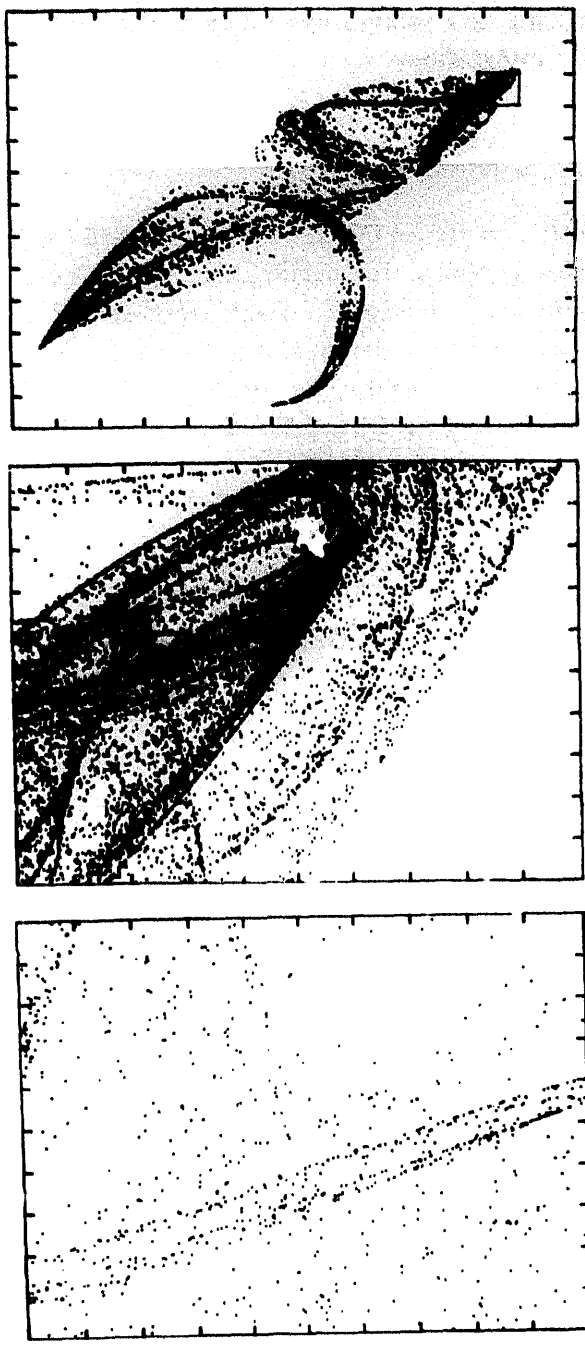

Fig. 6. See the caption to fig. 4, and table I. The delay parameter $\tau = 23.8$, and $D_F > 1.8$. (See caption of table I.) Fig. 6a contains 10,000 points; (b) and (c) were constructed using 200,000 crossings of the section.

Notice that in fig. 6 pronounced sheetlike structures are present. It appears as though most of the points lie on sheets, but a few of them "diffuse" outward to fill the section. (Compare to fig. 5.) Thus, the cross sections indicate that the Kaplan–Yorke conjecture correctly predicts the dimension, but the presence of only two nonnegative exponents preserves qualitative aspects of the sheetlike character of the attractor.

When τ is raised to 30 (fig. 7), there are two positive exponents (three non-negative), and the dimension is the order of 3.6. Notice that any sheet structure present is very blurred; the attractor is filled in much more uniformly than it is in fig. 6.

From the results of table I, and the qualitative features seen in these cross sections, it is clear that the conjecture of Mori (eq. (10)) is not correct for these high dimensional attractors. The conjecture of Kaplan and Yorke (eq. (9)) agrees with our numerical experiments to within the ability of the experiments to test it. It would, however, be worthwhile to perform these computations with more data at higher resolution.

For attractors of dimension greater than three, cross sections tend to all look like scatter plots, and the value of a cross section in visualizing the structure of an attractor and computing the dimension diminishes. It is for these higher dimensional attractors that the Kaplan–Yorke conjecture, together with a computation of the spectrum of Lyapunov exponents, becomes indispensable to determine the dimension of an attractor.

9. Computing Lyapunov exponents for delay equations

As mentioned in section 7, the state of a differential-delay equation (13) is determined by the function x on the interval $[t, t-\tau]$. This function can be approximated by N samples taken at intervals $\Delta t = \tau/(N-1)$. These N samples can equivalently be thought of as the N variables of an N-dimensional discrete mapping,

$$(x_1, \ldots, x_{N-1}, x_N) = (x(t-(N-1)\Delta t), \ldots, x(t-\Delta t), x(t)). \quad (15)$$

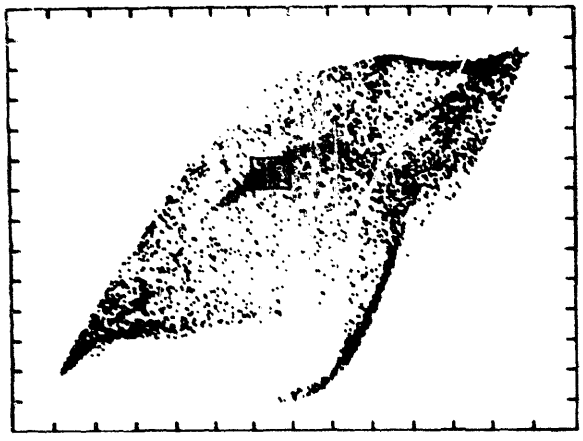

a

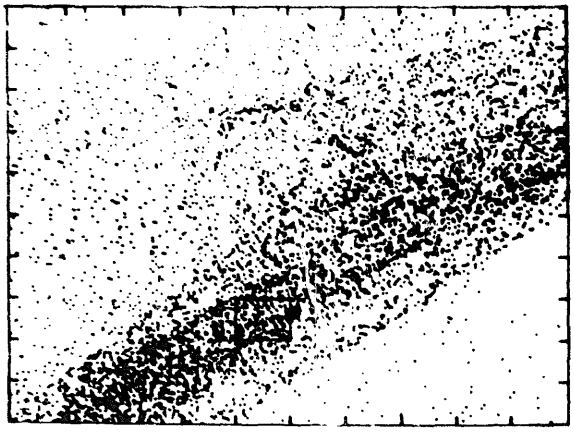

b

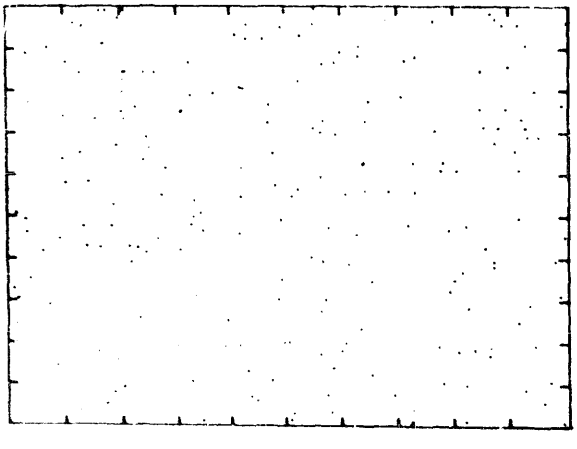

c

Fig. 7. See the caption to fig. 4, and table 1. The delay parameter $\tau = 30$, and $D_F > 1.94$. Fig. 7a contains 5000 points; (b) and (c) were constructed using 100,000 crossings of the section.

Choosing any integration scheme, for example, Euler integration,

$$x(t + \Delta t) = x(t) + F(x, x_\tau)\Delta t, \tag{16}$$

where $x_\tau = x(t - \tau)$, eq. (15) is reduced to an N-dimensional iterated map, $x(k + 1) = G(x(k))$. (k labels the iteration.) Each iteration of the map G corresponds to N timesteps Δt of the continuous equations, i.e. each iteration of G moves the system forward by time $\tau + \Delta t$. Using Euler integration, the map G is defined as follows:

$$\begin{aligned} x_1(k + 1) &= x_N(k) + F(x_N(k), x_1(k))\Delta t, \\ x_2(k + 1) &= x_1(k + 1) + F(x_1(k + 1), x_2(k))\Delta t, \\ &\vdots \\ x_N(k + 1) &= x_{N-1}(k + 1) + F(x_{N-1}(k + 1), x_N(k))\Delta t. \end{aligned} \tag{17}$$

To compute the Lyapunov exponents it is necessary to follow the evolution of small volumes. One method by which this can be done is to compute a reference trajectory, and simultaneously compute trajectories that are separated from the reference trajectory by a small amount. Alternatively, a set of infinitesimal separation vectors δx which define an infinitesimal volume element evolves according to

$$\delta x(k + 1) = \sum_{i=1}^{N} \frac{\partial G(x(k))}{\partial x_i(k)} \delta x_i(k). \tag{18}$$

To avoid the numerical problems associated with computing adjacent trajectories, eq. (18) can be used to compute the evolution of infinitesimal separations directly. When eq. (18) is applied to eq. (15), and recast as a continuous equation, it becomes

$$\frac{d\delta x}{dt} = \frac{\partial F(x, x_\tau)}{\partial x} \delta x + \frac{\partial F(x, x_\tau)}{\partial x_\tau} \delta x_\tau. \tag{19}$$

This equation can be solved using any convenient integration scheme. We use a Runge-Kutta algorithm.

The small separations δx represent a difference between two functions, or, equivalently, a small separation between two infinite-dimensional vectors. For convenience we will refer to them as *separation functions*.

Note on notation: $\delta x^i_j(k)$ denotes the jth coordinate of the ith separation function on the kth iteration, of the simulated system. For an N-dimensional simulation, there are N separation functions, corresponding to N Lyapunov exponents, and $1 < i, j < N$. The tilde $\underset{\sim}{\delta x}^i(k)$ denotes the collection of all N coordinates of a discretized separation function, i.e. the N-dimensional vector approximating a continuous separation function. A continuous separation function (in the limit $N \to \infty$) will be written δx^i.

Our numerical procedure to compute Lyapunov exponents, which is an adaptation of techniques used in finite dimensions [12, 13], proceeds as follows: For each exponent λ_i to be computed, arbitrarily select an initial separation function $\underset{\sim}{\delta x}^i(0)$. Integrate for a time τ, and renormalize $\underset{\sim}{\delta x}^i(1)$ to have length one. Using a Gram–Schmidt procedure, orthonormalize the second function relative to the first, the third relative to the second, and so on. Repeat this procedure for L iterations, and compute

$$\lambda_i = \frac{1}{L\tau} \sum_{k=1}^{L} \log \frac{\|\underset{\sim}{\delta x}^i(k)\|}{\|\underset{\sim}{\delta x}^i(k-1)\|}. \tag{20}$$

For L large enough, we find numerically that the values of λ_i converge. Note that we are arbitrarily choosing the Euclidean metric to define distance in the phase space

$$\|\underset{\sim}{\delta x}\| = \left(\sum_{j=1}^{N} \delta x_j^2\right)^{1/2} \tag{21}$$

If the attractor is a stable fixed point, then λ_i are the real parts of the eigenvalues of the linear part of F, and the separation functions are a real set of eigenfunctions. If the attractor is chaotic, however, each separation function varies chaotically with time, and the separation functions are no longer the eigenfunctions of the linearized problem.

The separation functions may be used to estimate the initial rate of relaxation of an arbitrarily chosen initial condition onto the attractor. If an initial function x_0 is expanded in terms of a set of separation functions,

$$x_0 = \sum_i k_i \delta x^i, \tag{22}$$

then $k_i\lambda_i$ gives a very rough estimate of the initial rate of relaxation of each component onto the attractor (for negative λ_i).

A few examples of separation functions are shown in fig. 8. Notice that separation functions of higher index i vary more rapidly than those of lower index. The results of several tests indicate that the ith function always has the order of i inflections.

10. Experimental results: exponents, dimension, and entropy

Figs. 9 and 10 summarize the results of our numerical computations of the spectrum of Lyapunov exponents. Fig. 9 shows the spectrum of the largest Lyapunov exponents, i.e. λ_i as a function of i, at each of three fixed parameter values. Fig. 10 shows each of the four largest exponents as the parameter τ is varied from 14 to 40.

We will use the Kaplan–Yorke conjecture, eq. (9), to construct the following plots of the Lyapunov dimension (which we assume corresponds to the information dimension) as a function of the parameter τ. The dimension as a function of τ is plotted in fig. 11, for τ between 15 and 40. For $\tau < 16.8$, the attractor is a limit cycle, and the dimension is one. At $\tau = 16.8$ the period doubling sequence accumulates, and the

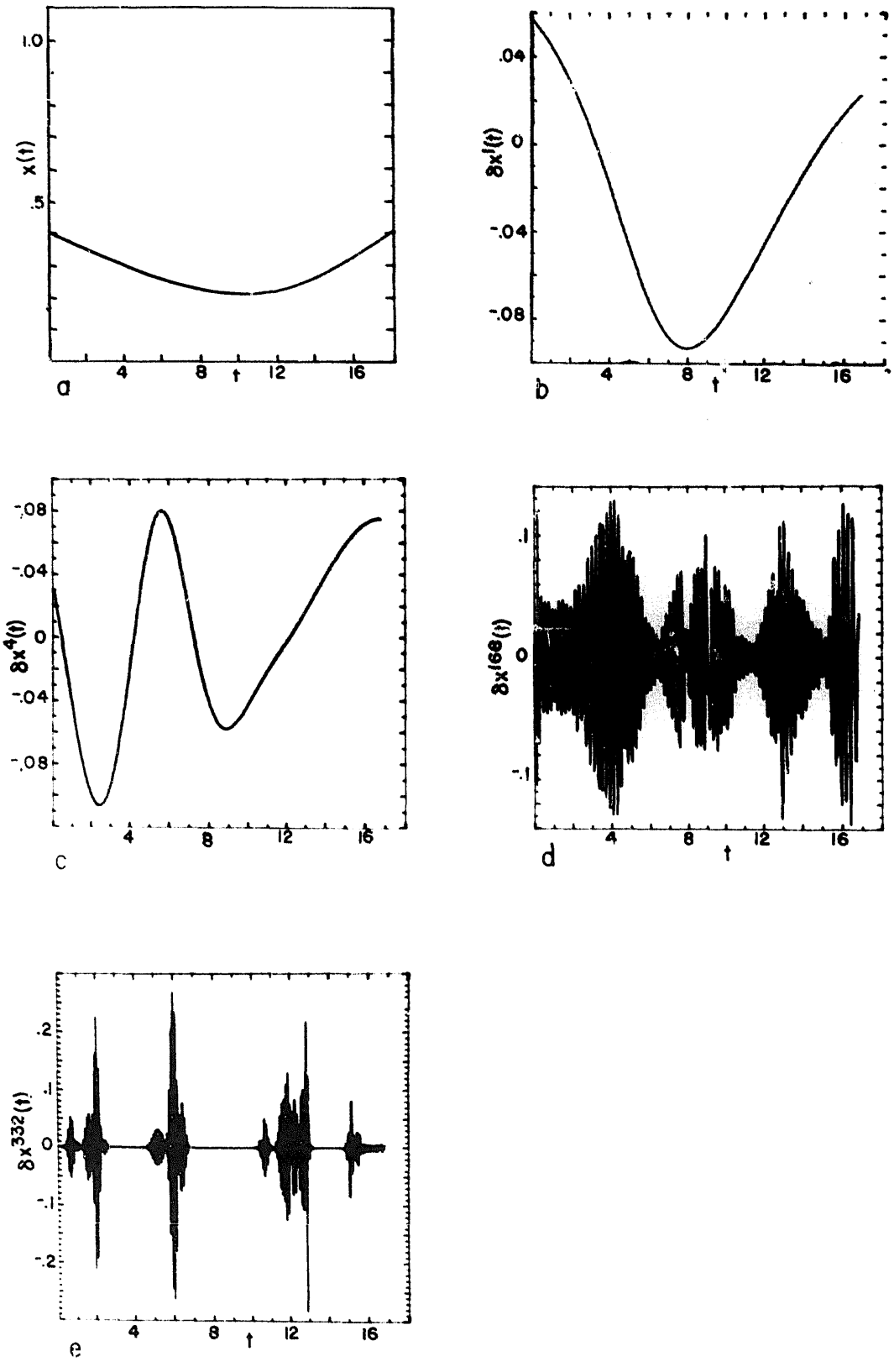
1.0
.5
x(t)
4
8
t
12
16
a
.04
0
-.04
-.08
δx¹(t)
b
-.08
-.04
0
-.04
-.08
δx⁴(t)
c
.1
0
-.1
δx¹⁶⁶(t)
d
.2
.1
0
-.1
-.2
δx³³²(t)
e

Fig. 8(a)–(e)

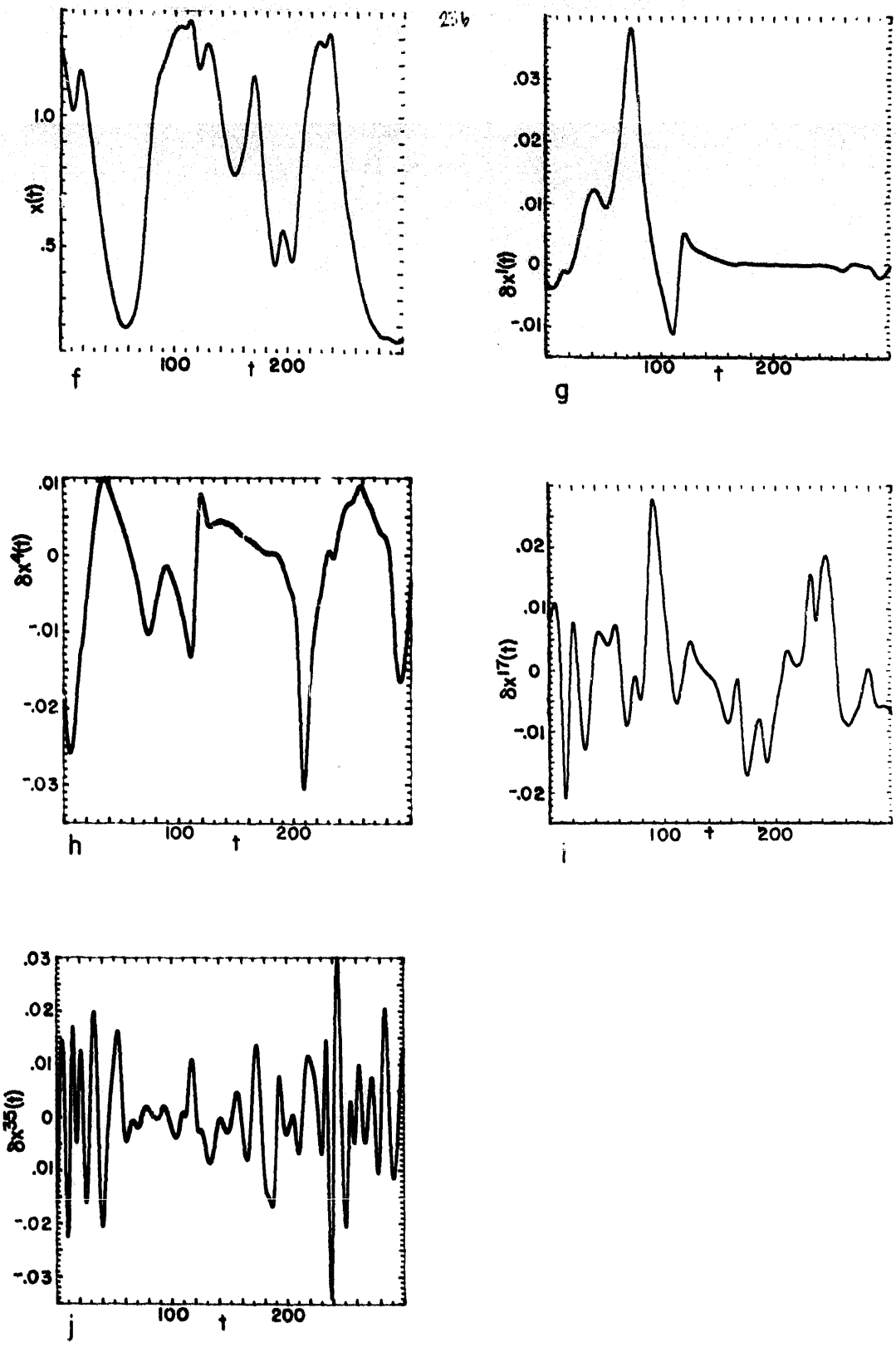

Fig. 8. Representative portions of time series $x(t)$, and representative portions of a few of the separation functions δx^i over an interval of length τ. For (a)–(e), $\tau = 16.8$ and $N = 336$. For (f)–(j) $\tau = 300$ and $N = 600$.

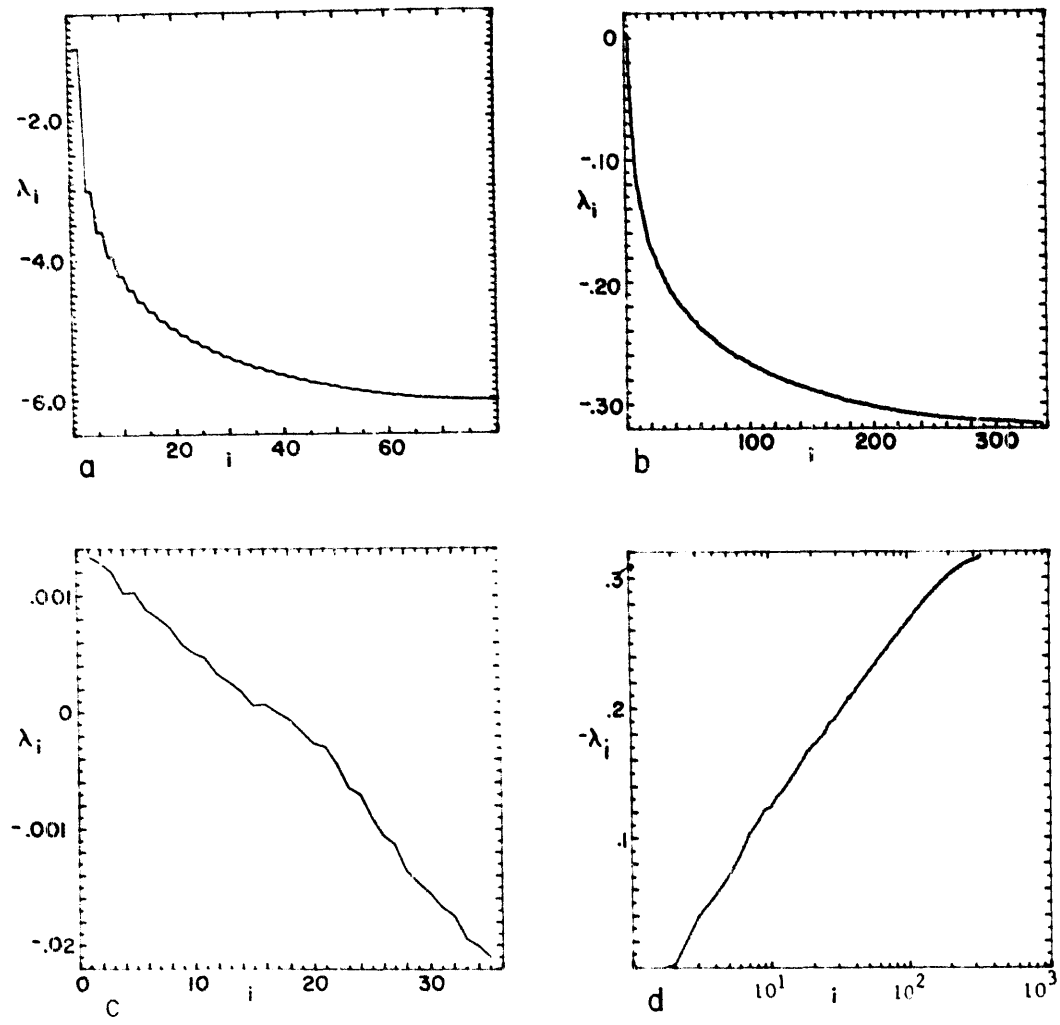

Fig. 9. The spectrum of Lyapunov exponents λ_i is plotted against i for eq. (14), at three values of the delay parameter τ. N is the number of grid points used for the discrete approximation i.e., the dimension of the simulation. (a) $\tau = 1$, $N = 80$. The attractor is a fixed point; in this case the spectrum of Lyapunov exponents shown here agree with the computed eigenvalues of the linearized problem. (b) $\tau = 16.8$, $N = 336$. This attractor is very near the accumulation parameter of a period doubling sequence. (c) $\tau = 300$, $N = 6000$. (See figs. 1d, 2d, and 3d.) Due to computational constraints, only the first 35 exponents are shown. (d) $-\lambda_i$ vs. log(i) for case (b), illustrating the asymptotic behavior of the exponents. (See eq. (22).)

dimension abruptly jumps to two, corresponding to the onset of chaotic behavior. As τ increases further, the dimension rises upward from two, and most parameter values show chaotic behavior, but at some there are stable limit cycles, causing the sharp downward jumps in $D_1(\tau)$ seen in fig. 11. This is similar to behavior seen in several finite dimensional examples. Note also that the shape of the graph of the largest Lyapunov exponent as a parameter is varied, fig. 10a, is qualitatively similar to that seen for the Rossler dynamical system [44], the logistic equation [48], and the Lorenz equations [13].

A quantitative comparison reinforces the similarity in this parameter range to low dimensional examples: The computations of the Lyapunov exponents quoted in the text were made using natural logarithms, and dividing by time units in terms of the variable t of eq. (14). As argued by Shaw [14], however, more physically relevant units are bits per characteristic

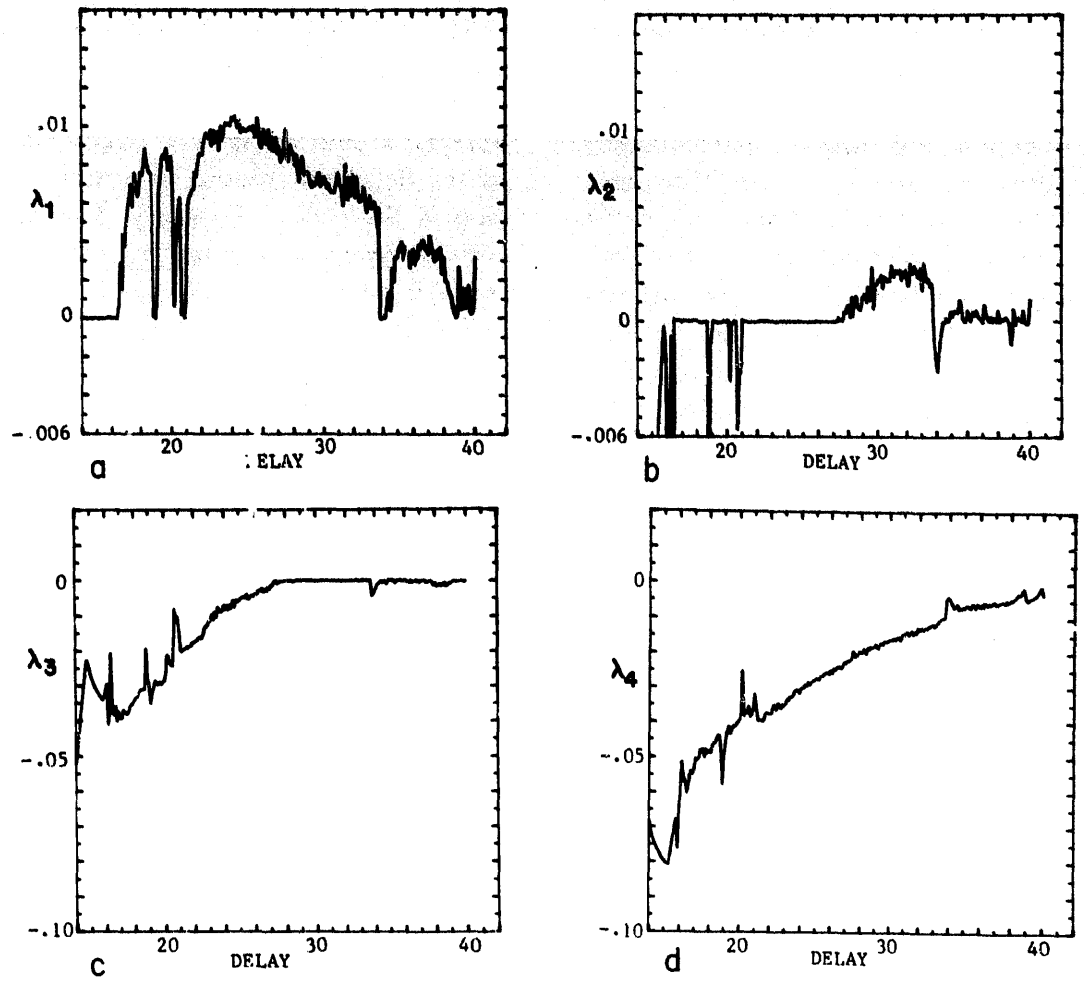

Fig. 10. The four largest Lyapunov exponents λ_i as the delay parameter τ varies from 14 to 40.

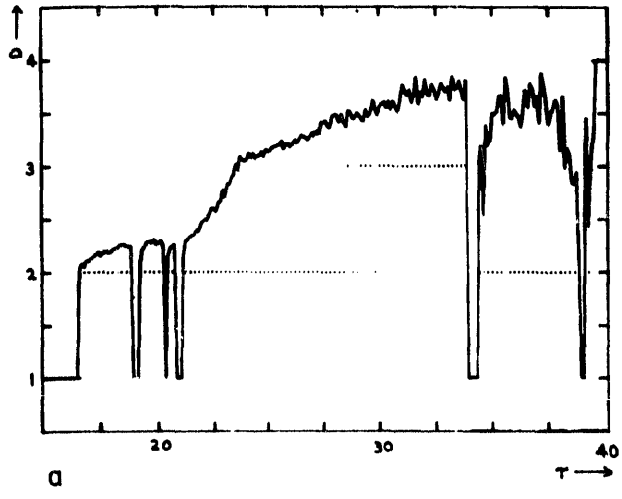

Fig. 11. The dimension as a function of τ for $\tau = 10$ to 40, at increments of 0.1. The information dimension, assumed to be given by the Kaplan–Yorke conjecture, eq. (9) is shown as a solid line. The number of non-negative Lyapunov exponents is indicated by a dotted line.

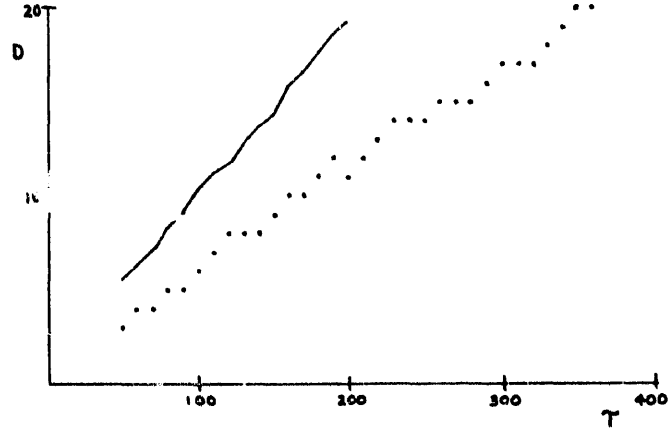

Fig. 12. The dimension as a function of τ for $\tau = 10$ to 400, in increments of 10. The solid line is the information dimension (same assumptions as fig 11). The dots indicate the number of non-negative Lyapunov exponents.

timescale. Using the fundamental period from the power spectrum of fig. 3a, calling this the characteristic timescale, and using logarithms in base two, the maximum value of the largest Lyapunov exponent (fig. 10a) is approximately one bit per characteristic timescale. This same behavior at the maximum is observed for the logistic equation [48], the Rossler equations [44], and the Lorenz equations [13]. This suggests that the chaotic attractor at $\tau = 24$, roughly where $\lambda_1 = 1$, makes roughly a two onto one fold every characteristic timescale. (See Shaw [14].)

For $\tau > 24$ however, the dimension exceeds three for many parameter values, and the qualitative behavior is unlike that seen in the lower dimensional examples mentioned above. Note that the dimension exceeds three while there are only two nonnegative exponents. The dimension continues to increase (note that the number of nonnegative exponents eventually jumps to three), until the dimension approaches four.

Fig. 12 shows a plot of the dimension as a function of τ, using coarser increments, and following τ from 50 to 400. Notice that the dimension increases at a fairly steady, nearly linear rate; at $\tau = 350$, the dimension is the order of 20. This might be interpreted as a steady transition to more "developed" chaos, as is borne out by the qualitatively more chaotic appearance of the time series in fig. 2b as compared with fig. 2d.

These results are in agreement with the predictions of Ruelle and Takens [2], in that no quasiperiodic tori of dimension greater than two are observed, in contrast to the behavior suggested by Landau [3]. The transition to "turbulence" begins with the appearance of a chaotic attractor, followed by a sequence of chaotic attractors of increasingly higher dimension.

One might ask: Just how steady is the transition to chaos? The results shown here suggest the following conclusion: As the delay parameter is varied, a sampling of parameter values shows the dimension changing sharply by as much as two or three. For low values of the delay parameter, where the dimension is the order of two, these sharp changes cause sharp changes in the qualitative properties of the attractor; for example, a chaotic attractor may become a limit cycle. For large values (e.g. 20) of the delay parameter, in contrast, the dimension is the order of twenty. The dimension is still observed to change by values of two or three, but the relative change in dimension, and also in qualitative behavior, is much smaller. As one might expect, the qualitative nature of high dimensional chaos appears more stable to changes of the parameters than the low dimensional chaos.

It is perhaps surprising that a plot of the sum of nonnegative exponents, fig. 13a, reveals that, although the dimension of the more delayed chaotic attractors is considerably larger, the metric entropy is approximately the same. To achieve this, all of the exponents, both positive and negative, get smaller in absolute value as the delay is increased (see fig. 8). In order for the metric entropy to remain constant while the dimension increases linearly, the positive exponents must decline as $1/\tau$. A plot of the largest exponent from $\tau = 50$ to $\tau = 400$ is shown in fig. 13b. Although the highly delayed attractors have a large dimension the local rates of expansion in each direction are quite small.

We can suggest a heuristic reason to connect the linear increase of the dimension as the delay parameter is varied to the constancy of the metric entropy. From the definition of embedding dimension, for a delay equation with an attractor of embedding dimension M, in principle the solution on the attractor on an interval of length τ is determined by only M of its values. If the embedding dimension increases linearly, so does the number of necessary samples per interval of length τ. Assuming that the observed linear growth of the information dimension implies linear growth of the embedding dimension, this implies that the number of samples needed per unit time interval is a constant. New samples are only required as a loss of

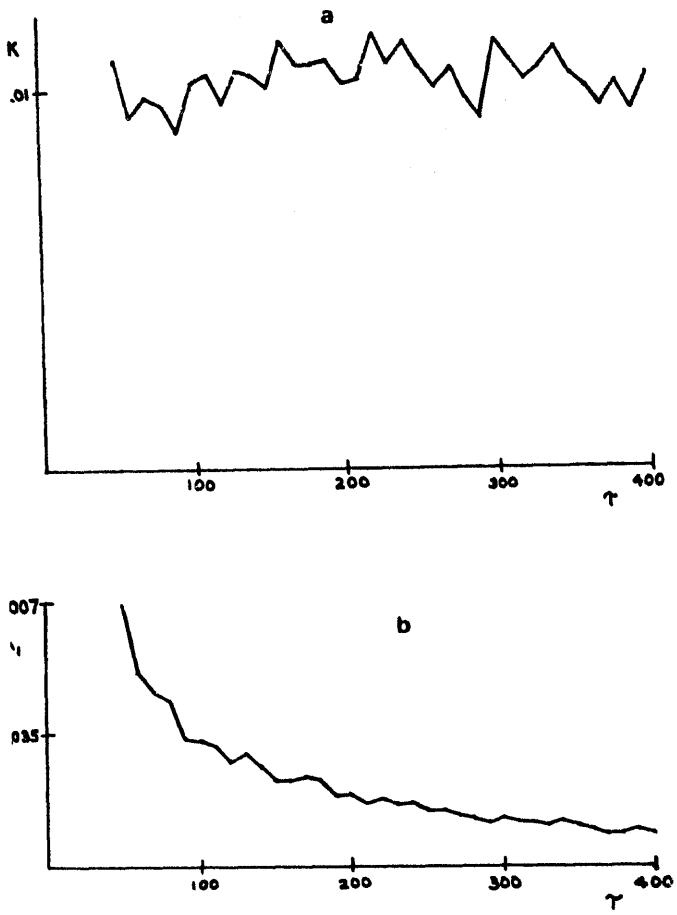

Fig. 13. (a) The metric (Kolomogorov–Sinai) entropy h_μ as a function of τ, from $\tau = 50$ to 400. Although the dimension increases significantly (see fig. 12), the metric entropy remains roughly constant. (There are fluctuations, but there is no systematic increase.) (b) The largest exponent λ_1 as a function of τ. In order to be consistent with the constancy of the metric entropy, and the smooth behavior of the spectrum of Lyapunov exponent observed in fig. 9, the positive exponents must decrease as $1/\tau$ for large τ.

information about the state of the system causes them to become necessary; this rate of loss of information is exactly the metric entropy. Thus, if the metric entropy is constant, one would expect that the number of samples needed per unit time would also be a constant. Thus, if the metric entropy is constant, according to this argument, the dimension should increase linearly with the delay time.

We doubt that the constancy of the metric entropy as a parameter is varied is a general property. The transition to chaos quite likely proceeds differently as other parameters are varied. We suspect that there is a general theorem for delay differential equations of this type that, in the limit of large delay time, links the sampling rate needed to determine the state on the attractor to the delay time τ and the metric entropy. Computational limitations have prevented our exploration of this question. We hope to investigate the effect of varying other parameters in a future study.

11. Asymptotic behavior of the spectrum of Lyapunov exponents

The Mackey–Glass equation is of the form

$$\dot{x} = g(x_\tau) - bx, \tag{23}$$

where b is a positive constant. By considering the divergence of an N dimensional proper simulation of this equation, and making use of the fact that a certain quantity approaches a constant as N goes to infinity, the asymptotic behavior of the Lyapunov exponents λ_i as $i \to \infty$ can be derived.

The average divergence of a discrete mapping is the average value of the logarithm of the Jacobian determinant. Let G_N be a N element approximation of eq. (19) in the form of eq. (15), such as the example given by eq. (17). The average divergence can then be computed to be

$$\langle \operatorname{div} G_N \rangle = \left\langle \sum_{j=1}^{N} \log |g'(x_j)\Delta t| \right\rangle, \tag{24}$$

where $\Delta t = \tau/(N-1)$. The average divergence of G_N is also equal to the sum of the Lyapunov exponents

$$\langle \operatorname{div} G_N \rangle = \sum_{i=1}^{N} \lambda_i. \tag{25}$$

(This may be used to check the computations of the Lyapunov exponents λ_i.)

Letting

$$\rho_N = \frac{1}{N}\left\langle \sum_{i=1}^{N} \log|g'(x_i)| \right\rangle, \tag{26}$$

eq. (24) can be rewritten

$$\langle \operatorname{div} G_N \rangle = N\rho_N + N \log \tau - N \log(N-1). \tag{27}$$

If the solution $x(t)$ is continuous, and Δt is made very small as N becomes large, then $x_{i+1} \approx x_i$. Assuming that $\log|g'(x(t))|$ is integrable, ρ_N will approach a constant value ρ as $N \to \infty$:

$$\rho = \lim_{T\to\infty} \frac{1}{T} \int_{t}^{t+T} \log|g'(x(s))|\, ds, \tag{28}$$

where $\langle \ldots \rangle$ is evaluated as a time average. Using eqs. (25) and (27), and approximating ρ_N as ρ, λ_i can be approximated for large values of i as

$$\lambda_i = \langle \operatorname{div} G_{i+1} \rangle - \langle \operatorname{div} G_i \rangle \approx \rho + \log \tau - \log i. \tag{29}$$

Since ρ and $\log \tau$ are constants, we are left with a logarithmic dependence of λ_i on i, which is confirmed by fig. 9d. The slight deviation from logarithmic behavior for i the order of N is due to the fact that the high order separation functions are not resolved accurately because of their many inflections (see fig. 8).

12. Comparison with a linearized analysis

The spectrum of Lyapunov exponents of an attractor that is a stable fixed point is simply the real part of the eigenvalues of the linearized problem. For a chaotic attractor, there is no such simple correspondence. Nevertheless, one can pick an *unstable* fixed point sitting on or near the chaotic attractor, compute the real parts of the eigenvalues of the linearized equation, and compare these numbers to the spectrum of Lyapunov exponents of the attractor. Since this latter procedure is so much easier to perform than a computation of the spectrum of Lyapunov exponents, a comparison is worthwhile to determine what qualitative information, if any, can be gained about the global stability of a dynamical system from a linearized calculation.

Assuming a solution of the form $\delta x(t) = Ae^{\lambda t}$, from eq. (19), λ is given by

$$\lambda = g'(x_p)\, e^{-2\pi} - b, \tag{30}$$

where x_p is the attracting fixed point. For the parameters $a = 0.2$, $b = 0.1$, and $c = 10$, the attractor is $x_p = 1$. If eq. (30) is separated into its real and imaginary parts, $\lambda = r + iw$, with a little rearrangement it becomes

$$r = -b - \frac{w}{\tan w\tau},$$

$$w(r) = [g'(x_p)^2\, e^{-2\pi} - (r+b)^2]^{1/2}. \tag{31}$$

This equation has an infinite number of discrete solutions. Marginal stability occurs when the largest solution is $r = 0$, i.e.

$$\tau = \frac{\tan^{-1}(-w(0)/b)}{w(0)} \tag{32}$$

which can be solved graphically (see fig. 14a.)

When $\tau > 4.53$, eq. (31) no longer correctly describes the stability of the attractor. It does, however, reproduce some of the correct qualitative features. The number of positive solutions to (31) is not the same as the number of positive exponents, but nevertheless the increase in the number of positive exponents is correctly predicted, as is their decrease in magnitude as τ is increased (see fig. 14b). Thus, a linear analysis is useful to give a very rough idea about the qualitative behavior as parameters are varied.

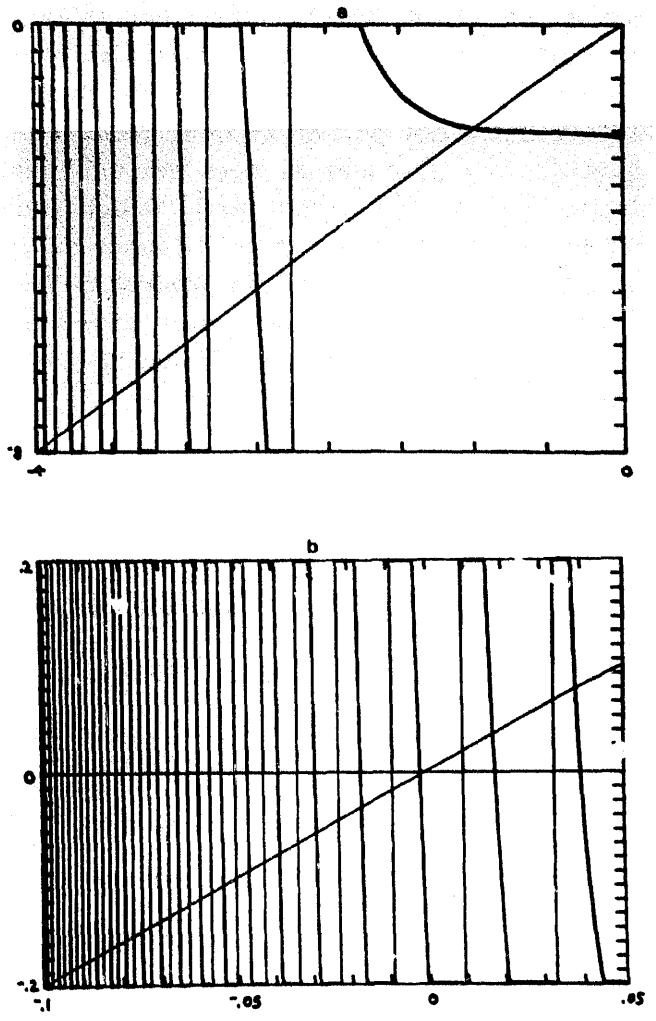

Fig. 14. The eigenvalues of eq. (14), linearized about the point $x_p = 1$, are given by the intersection of the curves with the diagonal line (See eq. (31).) (a) $\tau = 1$ and the attractor is a stable fixed point. In this case the set of linearized eigenvalues and the spectrum of Lyapunov exponents are the same (b) $\tau = 20$. The attractor is no longer a fixed point, but eq. (31) is solved as though it were to get an idea of the behavior of the exponents. There is some qualitative correspondence, but the quantitative behavior is quite different. (Compare with fig. 9.) Note the change of scale between (a) and (b).

13. Conclusions

We have approximated an infinite dimensional delay equation by a finite-dimensional mapping to enable computation of the spectrum of Lyapunov exponents. The low dimensional chaotic attractors of the delay equation studied here are qualitatively similar to those found in systems of ordinary differential equations. At large values of the delay parameter, however, we observed chaotic attractors with as many as 20 positive Lyapunov exponents. These high dimensional attractors have a fairly smooth exponential decay in their power spectrum, and their qualitative properties seem to be stable to changes in the delay parameter.

The transition to "turbulent" behavior begins with the appearance of a chaotic attractor (via a period doubling sequence), followed by chaotic attractors of increasingly higher dimension. Since no quasi-periodic tori are seen our results support the predictions of Ruelle and Takens. In addition, the transition to high dimensional chaos is fairly smooth, and proceeds with a nearly linear increase in the number of positive Lyapunov exponents as the delay parameter is increased. With a few assumptions, this last statement may be rephrased as follows: When transients have died away, the solution over any time interval may in principle be determined by a finite number of samples on that interval. After the dimension becomes large enough, the number of samples required per fixed time interval for the specification of the systems state is roughly a constant as the delay time τ is varied. Once the dimension is sufficiently large, the dimension increases smoothly at a linear rate as the delay parameter is varied. It is intriguing that the metric entropy remains roughly constant.

The conjecture of Kaplan and Yorke appears to be correct, at least within our ability to test it here. Their formula provides a good estimate of the dimension in terms of the Lyapunov exponents. Linear stability analysis about a point in function space gives qualitative, but not quantitative agreement with the computed spectrum of Lyapunov exponents. By making use of a quantity that is asymptotically invariant for discrete approximations to delay equations of the same type as the Mackey–Glass equation, the asymptotic behavior of the spectrum of

Lyapunov exponents is correctly predicted to be logarithmic.

Acknowledgments

I would like to specially thank Norman Packard for suggesting the discrete approximation method of computing Lyapunov exponents, and for his extensive suggestions and assistance in preparing the manuscript. I must also thank Rob Shaw for interesting me in delay equations, and John Guckenheimer and Jim Yorke for correcting technical errors in the original manuscript. Thanks are also due to Jim Crutchfield and Patrick Huerre for valuable conversations, to Yvain Treve for bringing refs. 5–8 to my attention, and to Ed Lorenz and Jim Curry for facilitating a visit to the National Center for Atmospheric Research, whose facilities made some of these computations possible. I would also like to thank Richard Kaplan and the University of Southern California Aerospace Engineering Department for their gracious hospitality and the use of their minicomputer. This work was supported by the Hertz Foundation.

Appendix A

Computational technique

These computations were done on computers at UC Santa Cruz (Basic, PDP 11/70), the National Center for Atmospheric Research (Fortran, Cray I), and the U. of Southern California (Fortran, PDP 11/55). Most of them were done in double precision. Although it is impossible to follow the trajectory on a chaotic attractor for very long with any accuracy, it is possible to compute accurate statistical averages. (See ref. 49.) The most significant errors in computing the Lyapunov exponents occur because (1) L in eq. (20) is too small, or (2) the timesteps Δt of the simulation are too coarse. For the majority of the computations, $\Delta t = 0.05$. For a few test cases, Δt was decreased to 0.025 and 0.01, and the results were within a few percent of those made with $\Delta t = 0.05$. The calculations were run until the fluctuations in the result were under one percent, typically 10^6 timesteps. All integrations were done with a Runge-Kutta algorithm. The power spectra shown in fig. 3 were computed using an FFT algorithm and a cosine bell data window.

References

[1] E.N. Lorenz, J. Atmos Sci. 2 (1963) 130.
[2] D. Ruelle and F. Takens, Comm. Math. Phys. 20 (1971) 167.
[3] L.D. Landau and E.M. Lifshitz, Fluid Mechanics (Pergamon, Oxford, 1959).
[4] Gollub and Swinney, Phys. Rev. Lett. 35 (1975) 927; Fenstermacher, Gollub, and Swinney, J. Fluid Mech. 94 (1979) 103. Walden and R.J. Donnelly, Phys. Rev. Lett. 42 (1979) 301. G. Ahlers and R.P. Behringer, Phys. Rev. Lett 40 (1978) 712.
[5] C. Foias and G. Prodi, Rend. Sem. Mat. Padova 3 (1967) 1.
[6] C. Foias and R. Temam, Comm. Pure and App. Math. 30 (1977) 149.
[7] O.A. Ladyzhenskaya, Soviet Physics (Doklady) 17 (1973) 647.
[8] O.A. Ladyzhenskaya, Journal of Sov. Math. 3 (1976) 458.
[9] J. Mallet-Paret, J. Diff. Eq., 22 (1976) 331.
[10] D. Ruelle, Characteristic Exponents and Invariant Manifolds in Hilbert Space, IHES preprint (1980).
[11] V.I. Oseledec, Trans. Moscow Math. Soc. 19 (1968) 197
[12] G. Bennetin, L. Galgani, and J. Strelcyn, Phys. Rev. A 14 (1976) 2338; also see G. Benettin, L. Galgani, A. Giorgilli and J. M. Strelcyn, Meccanica 15 (1980) 9.
[13] I. Shimada and T. Nagashima, Prog. Theor. Phys. Phys. 61 (1979) 1605.
[14] R. Shaw, Z. Naturforsch. 36a (1981) 80.
[15] J. Kaplan and J. Yorke, Functional Differential Equations and Approximation of Fixed Points, H.O. Peitgen and H.O. Walther, Eds. (Springer, Berlin, New York, 1979) p. 228.
[16] H. Mori, Prog. Theor. Phys. 63 (1980) 3.
[17] D. Russel, J. Hanson and E. Ott, Phys. Rev. Lett. 45 (1980) 1175.
[18] M.C. Mackey and L. Glass, Science 197 (1977) 287.
[19] D. Ruelle, Supplement to the Prog. Theor. Phys. 64 (1978) 339.

[20] R. Bowen and D. Ruelle, Inventiones Math. 29 (1975) 181.
[21] W. Hurewicz and H. Wallman, Dimension Theory (Princeton Univ. Press, Princeton, 1948).
[22] B. Mandelbrot, Fractals: Form Chance and Dimension (Freeman, San Fransisco, 1977).
[23] S. Smale, Bull. Amer. Math. Soc. 13, (1967) 747.
[24] M. Hénon, Comm. Math. Phys. 50 (1976) 69.
[25] J. Balatoni and A. Rényi, Publ. Math. Inst. of the Hungarian Acad. of Sci. 1 (1956) 9 (Hungarian). English translation, Selected papers of A. Rényi, Vol. 1 (Academiai Budapest, Budapest, 1976) p. 558. See also A. Rényi, Acta Mathematica (Hungary) 10 (1959) 193.
[26] D. Farmer, Information Dimension and the Probabilistic Structure of Chaos, Chapter 1, UCSC Doctoral Dissertation.
[27] J. Yorke, private communication.
[28] C. Shannon, Bell Tech. Jour. 27 (1948) 379.
[29] P. Billingsley, Ergodic Theory and Information (Wiley, New York, 1965).
[30] V.I. Arnold and A. Avez, Ergodic Problems of Classical Mechanics (Benjamin, New York, 1968).
[31] Ya. Sinai, Russ. Math. Surv. 166 (1972) 21.
[32] R. Bowen, Equilibrium States and the Ergodic Theory of Anasov Diffeomorphisms, (Springer, New York, 1975) p. 470.
[33] V.M. Alekseyev and M.V. Yakobson, Symbolic Dynamics and Hyperbolic Dynamical Systems, to appear in Physics Reports.
[34] P. Frederickson, J. Kaplan and J. Yorke, The Dimension of the Strange Attractor for a class of Difference Systems, preprint (1980).
[35] S. Goldstein, Entropy Increase in Dynamical Systems, [illegible] J. Math. Dept. preprint (1980).
[36] Ya. [illegible]sin, Uspekhi Mat. Nauk 32 (1977) 55.
[37] J. Crutchfield and N. Packard, UCSC preprint (1981).
[38] Computing the Lyapunov exponents of an infinite dimensional system via a finite dimensional approximation was suggested to me by unpublished calculations of the Lyapunov exponents of a partial differential equation by N. Packard.
[39] For a good introduction to center manifold theory, see J. [illegible]den, M. McKracken, The Hopf Bifurcation Theorem and its Applications, (Springer, New York, 1976).
[40] R. May, Annals of the NYAS 357 (1980) 267.
[41] Shibata, Math. Biosci. 51 (1980) 199.
[42] M. Feigenbaum, J. Stat. Phys. 19 (1978) 25.
[43] S. Grossman and S. Thomae, Z. Naturforsch 32a (1977) 1353.
[44] J. Crutchfield, D. Farmer, N. Packard, R. Shaw, G. Jones and R. Donnelly, Phys. Lett. 76A (1980) 1.
[45] E.N. Lorenz, Annals of N.Y. Acad. Sci. 357 (1980) 282.
[46] D. Farmer, Phys. Rev. Lett. 47 (1981) 179.
[47] D. Farmer, J. Crutchfield, H. Froehling, N. Packard and R. Shaw, Annals of N.Y. Acad Sci. 357 (1980) 453.
[48] J. Crutchfield, D. Farmer and B. Huberman, Fluctuations and Chaotic Dynamics, UCSC preprint (1980).
[49] G. Benettin, M. Casartelli, L. Galgani and J.M. Strelcyn, Nuovo Cimento 94B (1978) 183.